Growth and Characterizations of Superconducting FeSe Films on Flexible F-Mica Substrates

Liping Zhang, Juan Xu, Mingyang Qin, Ruozhou Zhang, Wei Hu, Yee Man Kwong, Chuqing Xia, Fung Tsz Fung, Jingsong Zhang, Jie Yuan, Beiyi Zhu, Jun Miao, and Kui Jin

***Abstract*—This article first reports the preparation of superconducting FeSe films on fluorophlogopite-mica (F-mica) substrates by the pulsed laser deposition technique. The quality of films is significantly improved by optimizing the deposition conditions, such as substrate temperature and laser energy. Through mechanical exfoliation of F-mica substrates, the films obtain excellent flexibility. After repeated bending in the atmosphere, the surface morphology and superconducting properties of these films substantially remain unchanged. Furthermore, we use a homemade device to apply different stains to the film and conclude that the superconducting transition temperature could be enhanced under compressive strain, whereas reduced under tensile strain. This article shows the great potential of FeSe superconducting films to integrate with future flexible electronic devices.**

***Index Terms*—FeSe superconducting film, flexible electronics, fluorophlogopite-mica (F-mica substrate).**

I. Introduction

SEEKING superconducting materials with appropriate physical properties has always been an important frontier field in condensed matter physics, which will facilitate the development of techniques such as lossless power transmission [1], [2], [3], magnetic levitation transportation [4], [5], and magnetic resonance imaging [6]. Beyond that, the superconductors can be used to fabricate high-performance electronic devices owing to low microwave surface impedance [7], [8], [9], [10] and Josephson effects [11], [12]. The iron-based superconductor has become an important family of high-temperature superconductors since its discovery in 2008 [13]. Among the iron-based superconductors, FeSe has the simplest structure and chemical composition. Besides, it has a high critical current density J_c [14] and a high upper critical magnetic field H_{c2} [15]. Especially, its superconducting transition temperature T_c can be adjusted in a wide range [16], [17], [18], [19], [20]. Therefore, FeSe has great potential in the application of superconductors [21], [22], [23].

Flexible superconducting films are highly in demand in engineering technologies, especially for future wearable or foldable electronics. However, current practical research works are mainly focused on superconducting films on rigid substrates. In other words, the information on the bending effect on superconducting thin films is relatively lacking [24], [25], [26], [27], which seriously limits the further development of flexible superconducting electronic technology. Therefore, the urgent task is to explore the growth of superconducting thin films on flexible substrates and study their superconducting properties before and after different deformations.

In this article, we choose fluorophlogopite-mica (F-mica) [$KMg_3Al(Si_3O_{10})F_2$] as the flexible substrate, which is a synthetic 2-D van der Waals layered material with atomically smooth surface, chemical inertness, thermal stability [28], [29], [30], and excellent optical and mechanical properties, and has been used to deposit a variety of oxides or nanocomposites [31], [32], [33], [34]. The pulsed laser deposition (PLD) technique is used to deposit FeSe thin films on F-mica substrates. Through systematically adjusting deposition conditions, we successfully grow superconducting FeSe films with $T_c \sim 6$ K, which exhibit well-textured features and superconductivity with $H_{c2} \sim 15$ T. In addition, the properties of the flexible superconducting thin films are stable and reversible after repeated bending and restoring. Furthermore, we use the homemade device to study the dependence of film's T_c on the strain and find that the superconductivity of FeSe benefits from the compressive strain.

II. Experiments

FeSe films with a thickness of ∼300 nm are deposited on F-mica substrates by PLD with a KrF excimer laser ($\lambda = 248$ nm). A target with a stoichiometric composition of $FeSe_{0.97}$ is used, and the distance between the target and the substrate is fixed at ∼50 mm. Before deposition, the chamber is evacuated to a high vacuum better than 1×10^{-6} torr. The growth parameters, such as laser energy, laser repetition rate, and substrate temperature,

Manuscript received 15 September 2022; revised 17 December 2022; accepted 6 January 2023. Date of publication 12 January 2023; date of current version 30 January 2023. This work was supported in part by the National Key Basic Research Program of China under Grant 2021YFA0718700, Grant 2018YFB0704102, Grant 2017YFA0303003, Grant 2017YFA0302902, Grant 2016YFA0300301, and Grant 2021YFA0718802; in part by the National Natural Science Foundation of China under Grant 11927808, Grant 11834016, Grant 118115301, Grant 119611410, Grant 11961141008, Grant 61727805, and Grant 11961141002; in part by the Key Research Program of Frontier Sciences, CAS under Grant QYZDB-SSW-SLH008 and Grant QYZDY-SSW-SLH001; in part by CAS Interdisciplinary Innovation Team, the Strategic Priority Research Program (B) of the Chinese Academy of Sciences under Grant XDB25000000 and Grant XDB33000000; in part by Beijing Natural Science Foundation under Grant Z190008; and in part by the Key-Area Research and Development Program of Guangdong Province under Grant 2020B0101340002. The work of Mingyang Qin was supported by the China Postdoctoral Science Foundation under Grant 2022M711497. This article was recommended by Associate Editor A. Augieri. *(Liping Zhang, Juan Xu and Mingyang Qin are co-first authors.) (Corresponding author: Mingyang Qin.)*

Please see the Acknowledgment section of this article for the author affiliations.

Color versions of one or more figures in this article are available at https://doi.org/10.1109/TASC.2023.3235827.

Digital Object Identifier 10.1109/TASC.2023.3235827

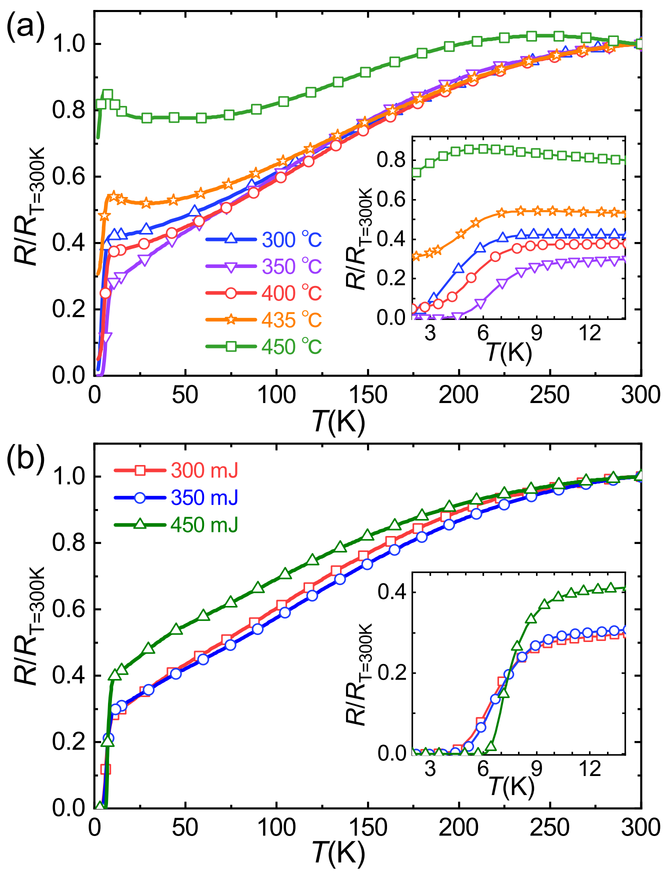

Fig. 1. Normalized resistance versus temperature (*R*–*T*) curves for FeSe/F-mica thin films. The films are deposited (a) at different substrate temperatures and (b) with different laser energies.

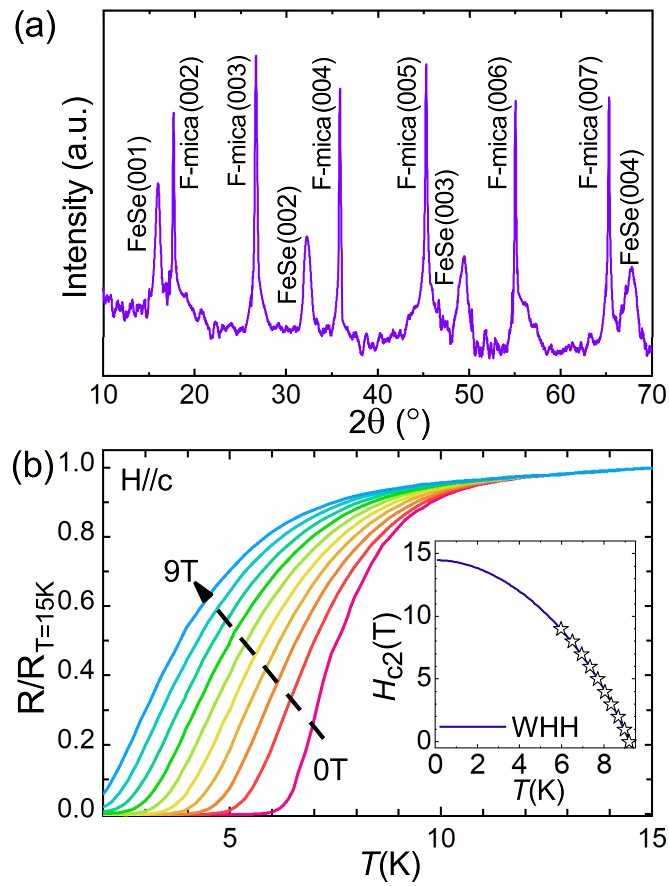

Fig. 2. (a) XRD spectra of θ–2θ scan for FeSe/F-mica, and (b) normalized *R*–*T* curves of the FeSe/F-mica film, measured under different applied magnetic fields. In the inset, the stars are the H_{c2} data extracted from (b) and the solid line shows the fit by WHH model [38]. The Maki parameter $\alpha = 3$, and the spin-orbit coupling constant $\lambda_{so} = 1$.

are adjusted according to the experimental requirements. X-ray diffraction (XRD, SmartLab 9 kW) and scanning electron microscopy (SEM, SU5000) are used to characterize the crystal structure and microstructure of films. The four-probe method is used to measure the temperature dependence of resistance (*R*–*T*) in the physical property measurement system (PPMS, Quantum Design).

III. Results and Discussions

The FeSe films are directly deposited on F-mica substrates with a thickness of 0.5 mm. To achieve high-quality films, many related deposition parameters have been studied. It is well known that the crystal structure of FeSe is sensitive to substrate temperature [35]. Therefore, we prepare the FeSe films at different substrate temperatures, ranging from 300 to 450 °C. Meanwhile, laser energy (300 mJ), repetition rate (4 Hz), and the annealing temperature (450 °C) keep constant. The *R*–*T* curves of these films are measured, as shown in Fig. 1(a). As the substrate temperature increases, the zero-resistance superconducting transition temperatures (T_{c0}) of films initially increase and then decrease. The highest $T_{c0} \sim 5$ K is reached when the substrate temperature is 350 °C. Hence, we choose the optimal grown temperature of 350 °C for the following depositions. Subsequently, we try the different laser energies, i.e., 300, 350, and 450 mJ, because the laser energy usually affects the plumpness and the stoichiometry of the plume [36]. Fig. 1(b) displays the *R*–*T* curves for the films with different laser energies, which shows the highest $T_{c0} \sim 6$ K (onset transition temperature of 9 K) is achieved using the laser energy of 450 mJ. Above all, we successfully fabricate superconducting FeSe films on F-mica substrates through careful adjustment of deposition conditions.

Furthermore, we characterize the crystal structure and electrical transport properties of the film with $T_{c0} \sim 6$ K. Fig. 2(a) shows the θ–2θ XRD patterns of the FeSe/F-mica. Only the FeSe (00*l*) peaks can be observed, indicating that although there exists a nonnegligible mismatch of in-plane lattice parameters between FeSe film and F-mica substrate [37], the FeSe film still displays *c*-axis orientation. This suggests that FeSe has a well-textured feature along the *c*-axis direction, as reported in previous work [26]. In addition, we estimate the *c*-axis lattice constant as ∼5.53 Å, similar to that of bulk FeSe [41], thus the lattice strain in our FeSe/F-mica is small. Fig. 2(b) shows the *R*–*T* curves of the film under different applied magnetic fields perpendicular to the film surface. The applied magnetic field H changes from 0 to 9 T and the interval ΔH is 1 T. It is noted that T_{c0} of the FeSe film gradually decreases with the increase of the magnetic field, but the film keeps superconducting transition even if the applied magnetic field is up to 9 T. Thus, we extract $H_{c2}(T)$ of the FeSe/F-mica using 90% of the normal-state resistance of the film. Then, the Werthamer–Helfand–Hohenberg (WHH) formula [38]

$$-H_{c2}(0) = 0.7T_c dH_{c2}/dT\,|T_c \quad (1)$$

is employed to fit $H_{c2}(T)$, which gives that $H_{c2}(0)$ of FeSe/F-mica is 14.5 T, as shown in the inset of Fig. 2(b). Although the out-of-plane upper critical magnetic field of FeSe/F-mica is relatively low [16], both T_{c0} and crystal structures are comparable to that of FeSe films on MgO, $LaAlO_3$, and other rigid crystal substrates [35]. We also believe that the film quality could be further improved by optimizing the deposition conditions.

The main purpose of this article is to fabricate and study the flexible superconducting film. Considering the F-mica substrate exhibits a sheet/layered structure and the interlayer van der Waals interaction is weak, it is possible to peel off the overlayer from F-mica creating an unconstrained or free-standing flake [37]. In addition, the F-mica usually has good flexibility when its thickness is less than 20 μm [39]. Therefore, we use the mechanical exfoliation method to cleave the F-mica substrate with a thickness of 0.5 mm into thin flakes of ~10 μm. The picture of the exfoliated sample is shown in Fig. 3(a), from which we can see that the FeSe/F-mica could be easily bent. We then repeatedly bend the sample with the homemade device (over 100 times in different directions and the maximum strain is ~0.46%) and compare its physical properties with that of the pristine. Fig. 3(b) and (c) show the surface morphology of the pristine and after-bending samples, respectively. It is found that the after-bending FeSe/F-mica does not display obvious wrinkles or cracks, indicating the good ductility of FeSe. In fact, the surface morphology has been checked on different film spots with different magnifications. In addition, it could be seen from the SEM micrographs that the FeSe film deposited on F-mica is dense. Fig. 3(d) and (e) show the XRD patterns and *R*–*T* curves of the pristine and after-bending samples, respectively. We find that both the crystal structure and the electrical transport property are barely affected by mechanical exfoliation and repeated bending. Note that there are three peaks corresponding to the impurity phases, which may come from the nonoptimal growth conditions and result in a lower T_{c0} of the sample [35], [36], [42]. All these results suggest that the mechanical characteristics, crystalline structures, and superconducting properties of the flexible FeSe film are stable under bending, which is promising for future flexible superconducting devices.

As a matter of fact, our flexible superconducting FeSe film provides a good platform for investigating the response of superconductivity to the applied strain [24], [40]. Fig. 4(a) shows the schematic of different bending configurations, with the flex-out and flex-in corresponding to the tensile and compressive strain, respectively [37]. When the curvature radius *R* is much larger than the sample thickness *t*, the magnitude of applied strain ε could be calculated by $\varepsilon = t/2R$ [24], [43]. That suggests that the smaller *R* is, the larger ε will be. In our experiments, the flexible FeSe/F-mica sample is attached to a beryllium copper shrapnel (the thickness is ~100 μm) with excellent elasticity

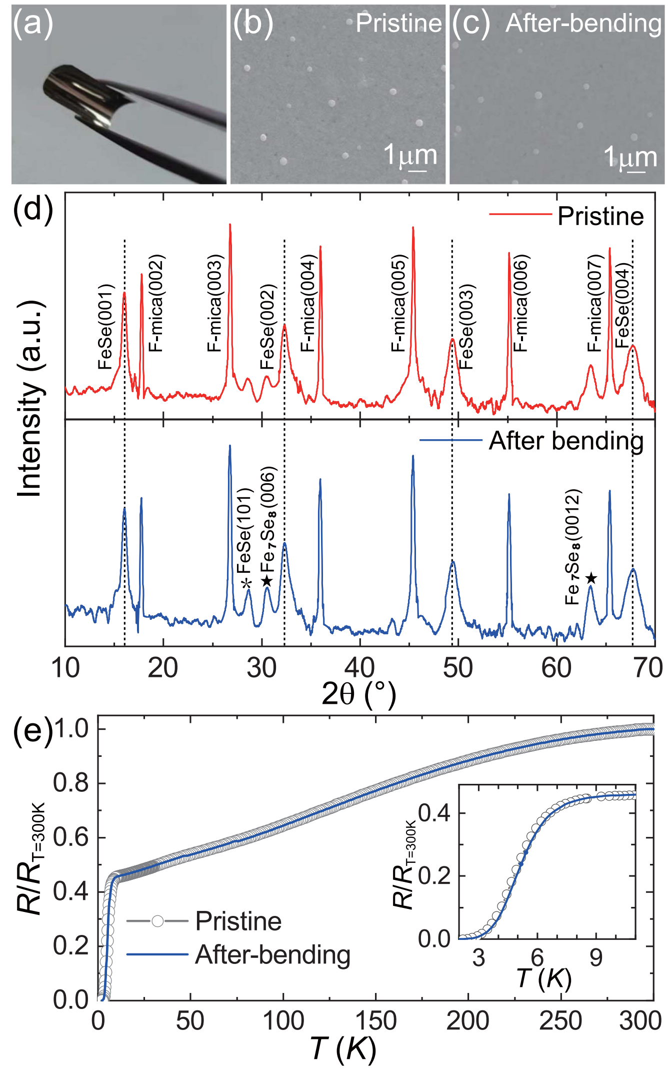

Fig. 3. Microstructure, crystalline structure, and electrical transport properties for the pristine and after-bending FeSe/F-mica film. (a) Picture of the exfoliated sample with bending condition. (b) SEM micrograph of the pristine film. (c) SEM micrograph of the after-bending film. (d) Out-of-plane XRD spectra of θ–2θ scan of the pristine and after-bending film. The asterisk symbol marks the FeSe(101) peak, and the star symbols mark the $Fe_7Se_8(006)$ and $Fe_7Se_8(0012)$ peaks. (e) Normalized *R*–*T* curves of the pristine and after-bending film.

and thermal conductivity [see Fig. 4(b)]. To make sure that the strain could be effectively applied to the FeSe film, we mounted the FeSe/F-mica onto the middle of copper shrapnel. Obviously, *R* becomes smaller with the decrease of *h*. In other words, the strain ε is larger for a shorter *h*. Then, the *R*–*T* curves of the sample are measured under different values of ε, as shown in Fig. 4(c). For the flex-out mode, the sample T_c decreases to 5.2 K and 5.0 K for $h = 23.7$ mm ($\varepsilon = 0.39\%$) and $h = 23.4$ mm ($\varepsilon = 0.40\%$), respectively, indicating that the tensile strain will suppress T_c. In contrast, for the flex-in mode corresponding to compressive strain ($h = 22.8$ mm, $\varepsilon = -0.41\%$), T_c is raised to ~6.5 K from the initial 5.3 K. Therefore, the tensile (positive)/compressive (negative) strain is unfavorable/conducive to the superconductivity of FeSe films. We note that Chen's group [24] also reported similar results where the superconductivity of

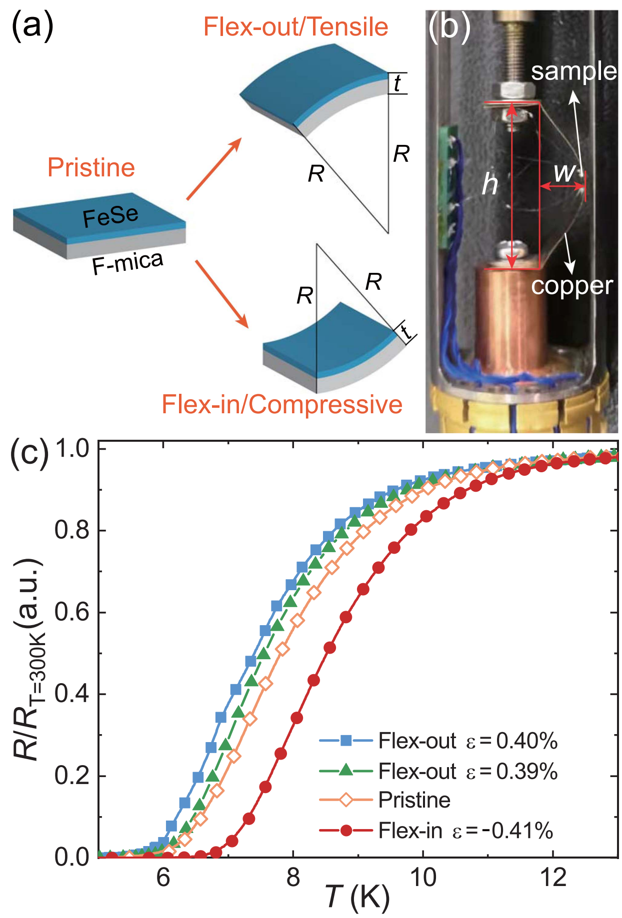

Fig. 4. (a) Schematics of both flex-in and flex-out bending modes. (b) Optical image of a homemade device, which is used to apply strain to the FeSe/F-mica in PPMS. (c) Normalized R–T curves of FeSe/F-mica in flex-in and flex-out bending conditions. Values of strain are estimated using $\varepsilon = t/2R$ and $R = (h^2+4w^2)/8w$, where h and w are geometrically explained in (b). ε is positive and negative for the flex-out and flex-in modes, respectively.

FeSe thin flakes on flexible polyethylene terephthalate substrates could be widely tuned through changing applied strains (T_c changes $\sim$2.8 K under a strain of $\sim -0.63\%$, in agreement with our results). This shows that the flexible superconductor is promising for investigating the mechanism of high-temperature superconductivity (see [24] and references therein).

V. Conclusion

The superconducting FeSe/F-mica films with $T_c \sim 6$ K are successfully prepared by the PLD technique with a substrate temperature of 350 °C and a laser energy of 450 mJ. After mechanical exfoliation of F-mica substrates and multiple bending of samples, the surface morphology, crystalline structure, and superconducting properties of flexible FeSe films keep almost unchanged, indicating that FeSe is a good candidate material for future flexible superconducting devices. Furthermore, we used our homemade device to investigate the response of the superconductivity of FeSe films to the applied strains. It is found that T_c will be enhanced under compressive strain and reduced under tensile strain, consistent with previous reports. Our study provides a new idea and method to prepare flexible superconducting thin films and shows the great potential of flexible FeSe films in the future applications of flexible electronic devices and the fundamental research on superconductivity.

Acknowledgment

Authors' Affiliations

Liping Zhang is with the School of Materials Science and Engineering, University of Science and Technology Beijing, Beijing 100083, China, and also with the Beijing National Laboratory for Condensed Matter Physics, Institute of Physics, Chinese Academy of Sciences, Beijing 100190, China (e-mail: lipingzhang@iphy.ac.cn).

Juan Xu, Wei Hu, and Beiyi Zhu are with the Beijing National Laboratory for Condensed Matter Physics, Institute of Physics, Chinese Academy of Sciences, Beijing 100190, China (e-mail: juanxu@iphy.ac.cn; huwei@iphy.ac.cn; beiyi.zhu@iphy.ac.cn).

Mingyang Qin is with the Beijing National Laboratory for Condensed Matter Physics, Institute of Physics, Chinese Academy of Sciences, Beijing 100190, China, and also with the Department of Materials Science and Engineering, Southern University of Science and Technology, Shenzhen 518055, China (e-mail: qinmy@sustech.edu.cn).

Ruozhou Zhang and Jingsong Zhang are with the Beijing National Laboratory for Condensed Matter Physics, Institute of Physics, Chinese Academy of Sciences, Beijing 100190, China, and also with the School of Physical Sciences, University of Chinese Academy of Sciences, Beijing 100049, China (e-mail: ruozhouzhang@iphy.ac.cn; zhangjingsong19@mails.ucas.ac.cn).

Yee Man Kwong is with the Department of Materials Science and Engineering, City University of Hong Kong, Hong Kong 999077, China (e-mail: ymkwong7-c@my.cityu.edu.hk).

Chuqing Xia is with the Semiconductor Technology Innovation Center (Beijing) Corporation, Beijing 050018, China (e-mail: xiachuqing.5@163.com).

Fung Tsz Fung is with the Department of Physics, City University of Hong Kong, Hong Kong 999077, China (e-mail: tszffung3-c@my.cityu.edu.hk).

Jie Yuan is with the Key Laboratory of Vacuum Physics, School of Physical Sciences, University of Chinese Academy of Sciences, Beijing 101408, China (e-mail: yuanjie@iphy.ac.cn).

Jun Miao is with the School of Materials Science and Engineering, University of Science and Technology Beijing, Beijing 100083, China (e-mail: j.miao@ustb.edu.cn).

Kui Jin is with the Beijing National Laboratory for Condensed Matter Physics, Institute of Physics, Chinese Academy of Sciences, Beijing 100190, China, also with the School of Physical Sciences, University of Chinese Academy of Sciences, Beijing 100049, China, and also with the Songshan Lake Materials Laboratory, Dongguan 523808, China (e-mail: kuijin@iphy.ac.cn).

References

[1] A. P. Malozemoff, "Second-generation high-temperature superconductor wires for the electric power grid," *Annu. Rev. Mater. Res.*, vol. 42, pp. 373–397, Mar. 2012, doi: 10.1146/annurev-matsci-100511-100240.

[2] C. Yao and Y. Ma, "Superconducting materials: Challenges and opportunities for large-scale applications," *iScience*, vol. 24, Jun. 2021, Art. no. 102541, doi: 10.1016/j.isci.2021.102541.

[3] S. R. Foltyn et al., "Materials science challenges for high-temperature superconducting wire," *Nature Mater.*, vol. 6, pp. 631–642, Sep. 2007, doi: 10.1038/nmat1989.

[4] F. Grilli, A. Morandi, F. D. Silvestri, and R. Brambilla, "Dynamic modeling of levitation of a superconducting bulk by coupled *H*-magnetic field and arbitrary Lagrangian-Eulerian formulations," *Supercond. Sci. Technol.*, vol. 31, no. 12, Oct. 2018, Art. no. 125003, doi: 10.1088/1361-6668/aae426.

[5] W. Yang, L. Quéval, and G. Ma, "Numerical studies of dynamic characteristics of a stack-type HTS maglev system based on H-formulation," *IEEE Trans. Appl. Supercond.*, vol. 32, no. 6, Sep. 2022, Art. no. 3602704, doi: 10.1109/TASC.2022.3160965.

[6] Y. Li and S. Roell, "Key designs of a short-bore and cryogen-free high temperature superconducting magnet system for 14 T whole-body MRI," *Supercond. Sci. Technol.*, vol. 34, no. 12, Oct. 2021, Art. no. 125005, doi: 10.1088/1361-6668/ac2ec8.

[7] M. Arzeo, F. Lombardi, and T. Bauch, "Microwave losses in YBCO coplanar waveguide resonators at low power and millikelvin range," *IEEE Trans. Appl. Supercond.*, vol. 25, no. 3, Jun. 2015, Art. no. 1700104, doi: 10.1109/TASC.2014.2364777.

[8] Z. F. Lin et al., "Enhancement of the lower critical field in FeSe-coated Nb structures for superconducting radio-frequency applications," *Supercond. Sci. Technol.*, vol. 34, no. 1, Nov. 2021, Art. no. 015001, doi: 10.1088/1361-6668/abc568.

[9] T. Kubo, "Multilayer coating for higher accelerating fields in superconducting radio-frequency cavities: A review of theoretical aspects," *Supercond. Sci. Technol.*, vol. 30, p. 2, Dec. 2016, Art. no. 023001, doi: 10.1088/1361-6668/30/2/023001.

[10] R. W. Ratston, "Microwave applications of superconducting electronics," *Supercond. Sci. Technol.*, vol. 4, 1991, Art. no. 386, doi: 10.1088/0953-2048/4/9/003.

[11] I. Kawayama, C. Zhang, H. Wang, and M. Tonouchi, "Study on terahertz emission and optical/terahertz pulse responses with superconductors," *Supercond. Sci. Technol.*, vol. 26, Jul. 2013, Art. no. 093002, doi: 10.1088/0953-2048/26/9/093002.

[12] R. L. Fagaly, "Superconducting quantum interference device instruments and applications," *Rev. Sci. Instrum.*, vol. 77, Oct. 2006, Art. no. 101101, doi: 10.1063/1.2354545.

[13] Y. Kamihara, T. Watanabe, M. Hirano, and H. Hosono, "Iron-based layered superconductor $La[O_{1-x}F_x]FeAs$ ($x = 0.05-0.12$) with $T_c = 26$ K," *J. Amer. Chem. Soc.*, vol. 130, pp. 3296–3297, Jan. 2008, doi: 10.1021/ja800073m.

[14] H. Lei et al., "Iron chalcogenide superconductors at high magnetic fields," *Sci. Technol. Adv. Mater.*, vol. 13, Dec. 2012, Art. no. 054305, doi: 10.1088/1468-6996/13/5/054305.

[15] P. Mele, "Superconducting properties of iron chalcogenide thin films," *Sci. Technol. Adv. Mater.*, vol. 13, 2012, Art. no. 054301, doi: 10.1088/1468-6996/13/5/054301.

[16] Y. Miyata, K. Nakayama, K. Sugawara, T. Sato, and T. Takahashi, "High-temperature superconductivity in potassium-coated multilayer FeSe thin films," *Nature Mater.*, vol. 14, pp. 775–779, Aug. 2015, doi: 10.1038/NMAT4302.

[17] J. Guo et al., "Superconductivity in the iron selenide $K_xFe_2Se_2$ ($0 \leq x \leq 1.0$)," *Physica Rev. B*, vol. 82, Nov. 2010, Art. no. 180520, doi: 10.1103/PhysRevB.82.180520.

[18] B. Lei et al., "Evolution of high-temperature superconductivity from a low-T_c phase tuned by carrier concentration in FeSe thin flakes," *Phys. Rev. Lett.*, vol. 116, Feb. 2016, Art. no. 077002, doi: 10.1103/PhysRevLett.116.077002.

[19] M. Burrard-Lucas et al., "Enhancement of the superconducting transition temperature of FeSe by intercalation of a molecular spacer layer," *Nature Mater.*, vol. 12, pp. 15–19, Jan. 2013, doi: 10.1038/NMAT3464.

[20] M. Qin et al., "Granular metallicity as a minimal normal state for superconductivity," *Physica Rev. B*, vol. 104, Nov. 2021, Art. no. 174511, doi: 10.1021/acsami.1c14451.

[21] W. Si et al., "High current superconductivity in $FeSe_{0.5}Te_{0.5}$-coated conductors at 30 tesla," *Nature Commun.*, vol. 4, Jan. 2013, Art. no. 1347, doi: 10.1038/ncomms2337.

[22] M. Putti et al., "New Fe-based superconductors: Properties relevant for applications," *Supercond. Sci. Technol.*, vol. 23, no. 3, Feb. 2020, Art. no. 034003, doi: 10.1088/0953-2048/23/3/034003.

[23] H. Hosono, K. Tanabe, E. Takayama-Muromachi, H. Kageyama, S. Yamanaka, and H. Kumakura, "Exploration of new superconductors and functional materials, and fabrication of superconducting tapes and wires of iron pnictides," *Sci. Technol. Adv. Mater.*, vol. 16, May 2015, Art. no. 033503, doi: 10.1088/1468-6996/16/3/033503.

[24] Z. H. Cheng et al., "Revealing the A_{1g}-type strain effect on superconductivity and nematicity in FeSe thin flake," *Chin. Phys. B*, vol. 30, no. 9, Aug. 2021, Art. no. 097403, doi: 10.1088/1674-1056/ac1efa.

[25] J. Huang, H. Wang, H. Wang, B. Zhang, X. Qian, and H. Wang, "Superconducting iron chalcogenide thin films integrated on flexible mica substrates," *IEEE Trans. Appl. Supercond.*, vol. 29, no. 5, Aug. 2019, Art no. 7500604, doi: 10.1109/TASC.2019.2906771.

[26] J. Huang, L. Chen, J. Jian, F. Khatkhatay, C. Jacob, and H. Wang, "A simplified superconducting coated conductor design with Fe-based superconductors on glass and flexible metallic substrates," *J. Alloys Compounds,* vol. 647, pp. 380–385, 2015, doi: 10.1016/j.jallcom.2015.06.109.

[27] R. Zhang et al., "Wafer-scale epitaxy of flexible nitride films with superior plasmonic and superconducting performance," *ACS Appl. Mater. Interfaces*, vol. 13, pp. 60182–60191, Dec. 2021, doi: 10.1021/acsami.1c18278.

[28] M. Yen, Y.-H. Lai, C.-Y. Kuo, C.-T. Chen, C.-F. Chang, and Y.-H. Chu, "Mechanical modulation of colossal magnetoresistance in flexible epitaxial perovskite manganite," *Adv. Funct. Mater.*, vol. 30, Jul. 2020, Art. no. 2004597, doi: 10.1002/adfm.202004597.

[29] J. W. McCauley, R. E. Newnham, and G. V. Gibbs, "Crystal-structure analysis of synthetic fluorophlogopite," *Amer. Mineralogist*, vol. 58, pp. 249–254, Jan. 1973.

[30] Q. Q. Ji et al., "Epitaxial monolayer MoS_2 on mica with novel photoluminescence," *Nano Lett.*, vol. 13, pp. 3870–3877, Jul. 2013, doi: 10.1021/nl401938t.

[31] W. L. Liu et al., "Mechanical strain-tunable microwave magnetism in flexible $CuFe_2O_4$ epitaxial thin film for wearable sensors," *Adv. Funct. Mater.*, vol. 28, Jan. 2018, Art. no. 1705928, doi: 10.1002/adfm.201705928.

[32] Y. Jing et al., "Weak antilocalization and electron-electron interaction in coupled multiple-channel transport in a Bi_2Se_3 thin film," *Nanoscale*, vol. 8, pp. 1879–1885, Dec. 2016, doi: 10.1039/C5NR07296D.

[33] J. Jiang et al., "Flexible ferroelectric element based on van der Waals heteroepitaxy," *Sci. Adv.*, vol. 3, Jun. 2017, Art. no. e1700121, doi: 10.1126/sciadv.1700121.

[34] C. Yang et al., "Fatigue-free and bending-endurable flexible Mn-doped $Na_{0.5}Bi_{0.5}TiO_3$-$BaTiO_3$-$BiFeO_3$ film capacitor with an ultrahigh energy storage performance," *Adv. Energy Mater.*, vol. 9, Mar. 2019, Art. no. 1803949, doi: 10.1002/aenm.201803949.

[35] Z. P. Feng et al., "Tunable critical temperature for superconductivity in FeSe thin films by pulsed laser deposition," *Sci. Rep.*, vol. 8, Mar. 2018, Art. no. 4039, doi: 10.1038/s41598-018-22291-z.

[36] Z. Feng et al., "High-throughput investigation of tunable superconductivity in FeSe films," 2019, doi: 10.48550/arXiv.1807.01273.

[37] Y. Bitla and Y.-H. Chu, "Micatronics: A new platform for flexible X-tronics," *FlatChem*, vol. 3, pp. 26–42, Jun. 2017, doi: 10.1016/j.flatc.2017.06.003.

[38] N. R. Werthamer, E. Helfand, and P. C. Hqhenberg, "Temperature and purity dependence of the superconducting critical field, H_{c2}.III. Electron spin and spin-orbit effects," *Physica Rev. B*, vol. 147, Jul. 1966, Art. no. 295, doi: 10.1103/PhysRev.147.295.

[39] W. Gao et al., "Flexible $PbZr_{0.52}Ti_{0.48}O_3$ capacitors with giant piezoelectric response and dielectric tunability," *Adv. Electron. Mater.*, vol. 3, May 2017, Art. no. 1600542, doi: 10.1002/aelm.201600542.

[40] M. Nakajima, Y. Ohata, and S. Tajima, "Control of band structure of FeSe single crystals via biaxial strain," *Phys. Rev. Mater.*, vol. 5, Apr. 2021, Art. no. 044801, doi: 10.1103/PhysRevMaterials.5.044801.

[41] F.-C. Hsu et al., "Superconductivity in the PbO-type structure α-FeSe," *Proc. Nat. Acad. Sci. USA*, vol. 105, pp. 14262–11464, Sep. 2008, doi: 10.1073/pnas.0807325105.

[42] H. Yang et al., "Preparation and characterization of high-quality FeSe single crystal thin films," *Acta Physica Sinica*, vol. 67, 2018, Art. no. 207416, doi: 10.7498/aps.67.20180940.

[43] Y. Wang et al., "Strain-sensitive magnetization reversal of a van der Waals magnet," *Adv. Mater.*, vol. 32, 2020, Art. no. 2004533, doi: 10.1002/adma.202004533.